Supporting Information

A new FRET probe for ratiometric fluorescence detecting mitochondria-localized drug activation and imaging endogenous hydroxyl radicals in zebrafish

Tao Deng,‡[a] Xiaojuan Wang,‡[a] Shengjun Wu,[a] Shiyou Hu,[a] Wei Liu,[b] Tongkai Chen,[b] Zhiqiang Yu,[c] Qin Xu*[a] and Fang Liu*[a]

[a] *Institute of Tropical Medicine and Artemisinin Research Center, Guangzhou University of Chinese Medicine, Guangzhou 510405, China*

[b] *Science and Technology Innovation Center, Guangzhou University of Chinese Medicine, Guangzhou 510405, China*

[c] *School of Pharmaceutical Sciences, Guangdong Provincial Key Laboratory of New Drug Screening, Southern Medical University, Guangzhou, 510515, China*

‡ *These authors contributed equally to this work.*

Corresponding author: Fang Liu, Email: fangliu@gzucm.edu.cn
Qin Xu, Email: xuqin@gzucm.edu.cn

1. Materials and methods

Chemicals were purchased from commercial sources, other reagents were AR grade and used without further purification unless otherwise indicated. Mito Tracker Green was purchased from Thermo Fisher Scientific (US). Xanthine oxidase was purchased from Solarbio (China). The distilled deionized water from a Milli-Q Plus system was used throughout the experiments. High-performance liquid chromatography (Agilent HPLC 1260, USA) and a reverse phase C18 column (250 x 4.6 mm) were used in case needed. Plate reading was performed by a Varioskan LUX plate reader (Thermo Fisher) supplied with SkanIt Software 4.1. UV-vis absorption spectra were recorded on a spectrophotometer TU-1900 (Persee, Beijing). ESI-MS was recorded by an Agilent 6420 LC/MS instrument. ^{1}H and ^{13}C NMR spectra were recorded on AVANCE III HD 400 MHz digital NMR spectrometer (Switzerland). Data was reported as follows: chemical shift, multiplicity (s = singlet, d = doublet, and m = multiplet), coupling constant (*J* values) in Hz and integration. High resolution mass (HRMS) was collected from the Maxis Impact HD Mass Spectrometer (Bruker). Cell and zebrafish imaging were evaluated with Leica confocal microscopy (TCS-SPE-II).

2. Experimental Section

2.1 Synthesis and characterizations

The compound **3** was synthesized according to a reported method [1].

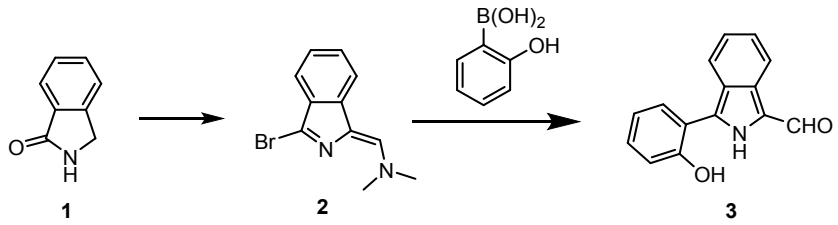

1 **2** **3**

Compound **2**: black solid (84%). ^{1}H NMR (400 MHz, $CDCl_3$) δ 7.53 – 7.49 (m, 2H), 7.26 – 7.22 (m, 1H), 7.18 – 7.13 (m, 2H), 3.62 (s, 3H), 3.27 (s, 3H). ESI $[M+H]^+$ m/z calcd. for [C11H12BrN2] 251.01, found 251.00 $[M+H]^+$.

Compound **3**: yellow solid (75%). ^{1}H NMR (400 MHz, d_6-DMSO) δ 13.39 (s, 1H), 10.24 (s, 1H), 9.91 (s, 1H), 8.18 (s, 1H), 7.82 (d, *J* = 8.4 Hz, 1H), 7.62 – 7.60 (m, 1H), 7.38 – 7.30 (m, 2H), 7.21 – 7.19 (s, 1H), 7.09 (d, *J* = 8.0 Hz, 1H), 7.02 – 6.98 (m, 1H). ESI $[M+H]^+$ m/z calcd. for [C15H12NO2] 238.08, found 238.10 $[M+H]^+$.

Synthesis of compound **4**

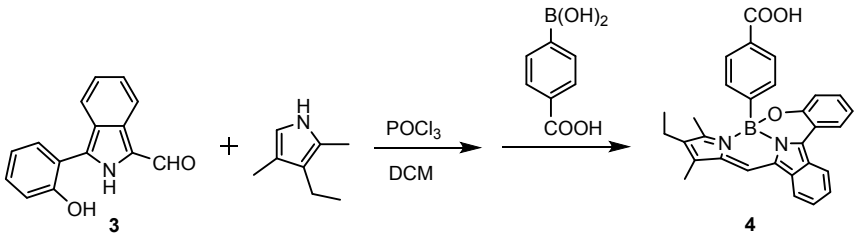

3 **4**

$POCl_3$ (0.01 mL, 0.13 mmol) was added to a dichloromethane solution (5 mL) of 2, 4-dimethyl-3-ethylpyrrole (32 mg, 0.26 mmol) at 0 °C. Then a solution of **3** (35 mg, 0.13 mmol) in dichloromethane (20 mL) was added dropwise to the reaction mixture at 0 °C. The reaction mixture was stirred at room temperature for 4 h. Then 4-carboxyphenylboronic acid (158 mg, 1.3 mmol) was added to the mixture at 0 °C. The reaction mixture was further stirred for 2 h at room

temperature and then the reaction solution 40 °C was heated for 5 hours. After evaporation of the solvent, the residual product was purified by silica-gel column chromatography (eluent: methanol/dichloromethane (v/v, 1:60) to give a blue powder of **4** (39 mg, 63%). ^{1}H NMR (400 MHz, $CDCl_3$) δ 8.03 (d, J = 8.5 Hz, 1H), 7.88 – 7.82 (m, 2H), 7.63 (d, J = 7.6 Hz, 2H), 7.43 – 7.39 (m, 1H), 7.36 – 7.32 (m, 2H), 7.2 – 7.21 (m, 4H), 6.91 – 6.87 (m, 1H), 2.36 (s, 3H), 2.31 – 2.26 (m, 2H), 2.19 (s, 3H), 0.97 – 0.93 (m, 3H). Mass spectrometry (ESI-HRMS, m/z): $[M+H]^+$ calcd. for $[C30H26BN2O3]^+$ 473.2036; found 473.2039.

Synthesis of compound **5**

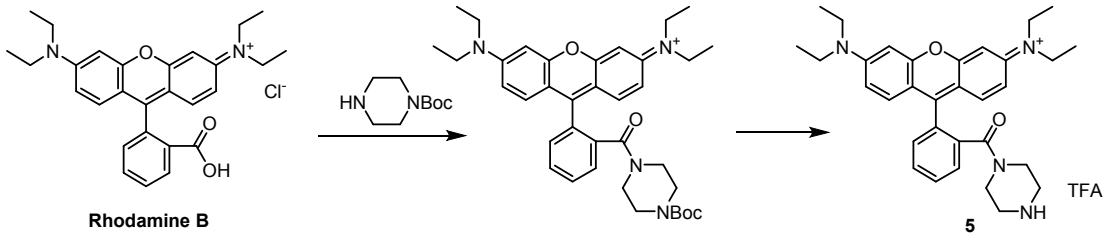

Rhodamine B **5**

***Tert*-butyl piperazine-1-carboxylate：** This compound was synthesized according to a reported procedure [2]. A white solid was achieved (90%). ^{1}H NMR (400 MHz, $CDCl_3$) δ 3.54 – 3.22 (m, 4H), 2.88 – 2.57 (m, 4H), 1.82 (s, 1H), 1.39 (s, 9H). ESI [M+H]+ m/z calcd. for [C9H19N2O2] 187.14, found 187.14 $[M+H]^+$.

Rhodamine-N-piperrazine-N-Boc: To the mixture of Rhodamine B (0.20 mmol) and DMF (5 mL), *tert*-butyl piperazine-1-carboxylate (0.41 mmol), EDC (0.41 mmol) and HOBt (0.25 mmol) were added. The mixture was stirred at room temperature. Reaction was monitored by TLC. Upon completion, reaction mixture was diluted with EtOAc and washed with water (3 × 30 mL). The organic phase was dried over Na_2SO_4 and concentrated under reduced pressure. The crude product was purified by silica gel chromatography using methanol/dichloromethane (v/v, 1:50) as the eluent to afford the desired compound as a pink solid (87 mg). Yield 80%. ^{1}H NMR (400 MHz, CD_3OD) δ 7.64 – 7.62 (m, 2H), 7.48 – 7.46 (m, 1H), 7.30 – 7.27 (m, 1H), 7.16 (s, 1H), 7.14 (s, 1H), 6.84 (d, J = 8.9 Hz, 2H), 6.73 (d, J = 1.8 Hz, 2H), 3.61 – 3.51 (m, 8H), 3.32 – 3.19 (m, 8H), 1.34 (s, 9H), 1.27 – 1.23 (m, 12H). ^{13}C NMR (100 MHz, CD_3OD) δ 168.17, 157.88, 155.80, 155.63, 154.62, 135.21, 131.84, 130.86, 130.36, 129.94, 129.89, 114.02, 113.46, 95.97, 80.37, 45.54, 27.18, 11.49. ESI $[M+H]^+$ m/z calcd. for [C37H48N4O4] 612.36, found 612.36 $[M+H]^+$.

Synthesis of compound **5**

Rhodamine-N-piperrazine-N-Boc (1 mmol) and TFA (3 mL) were stirred in DCM (7 mL) for 30 minutes. After removing solvent under vacuum, diethyl ether was added and centrifuged. The product compound **5** was directly used in next step without further purification (pink solid, 91% yield). ESI $[M]^+$ m/z calcd. for [C32H39N4O2] 511.31, found 511.40 $[M]^+$.

Synthesis of compound Rho-Bob (**6**)

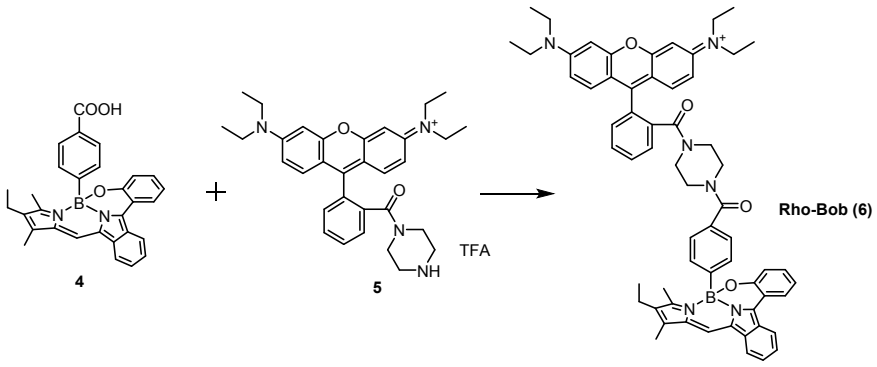

To the mixture of Compound **4** (0.08 mmol) and DMF (5 mL), compound **5** (0.11 mmol), EDC (0.16 mmol) and HOBt (0.11 mmol) were added. The mixture was stirred at room temperature. Reaction was monitored by TLC. Upon completion, reaction mixture was diluted with EtOAc and washed with water (3 × 30 mL). The organic phase was dried over Na_2SO_4 and concentrated under reduced pressure. The crude product was purified by silica gel chromatography using methanol/dichloromethane (v/v, 1:80) as the eluent to afford compound **6** as a blue solid (55 mg), Yield 71%. ^{1}H NMR (400 MHz, *d6*-DMSO) δ 8.35 – 8.24 (m, 2H), 8.16 (s, 2H), 7.70 – 7.59 (m, 4H), 7.50 – 7.42 (m, 3H), 7.26 (d, J = 8.2 Hz, 1H), 7.12 – 7.00 (m, 5H), 6.91 (s, 2H), 3.62 (d, J = 6.5 Hz, 8H), 3.23 (s, 8H), 2.43 (s, 3H), 2.39 – 2.33 (m, 2H), 2.29 (s, 3H), 1.18 – 1.15 (m, 12H), 1.02 – 0.98 (m, 3H). ^{13}C NMR (100 MHz, *d6*-DMSO) δ 169.75, 166.86, 157.41, 156.45, 155.97, 155.46, 150.62, 142.56, 135.56, 135.30, 134.59, 133.99, 133.77, 132.21, 132.11, 131.13, 131.13, 131.02 , 130.77, 130.36, 130.18, 130.15, 130.02, 129.56, 127.98, 127.14, 126.51, 126.46, 125.84, 123.94, 120.97, 120.77, 120.23, 118.62, 114.69, 113.38, 96.28, 45.78, 17.25, 15.13, 13.24, 12.81, 9.70. Mass spectrometry (ESI-HRMS, m/z): $[M]^+$ calcd. for $[C62H62BN6O4]^+$ 965.4920; found 965.4928.

Synthesis of compound **8** (DHA-TPP)

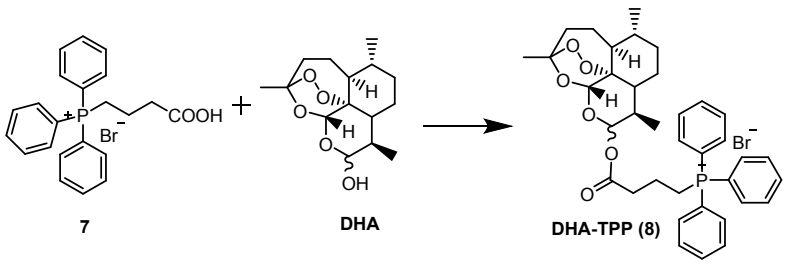

To the mixture of compound **7** (0.17 mmol) and DMF (5 mL), DHA (0.21 mmol), EDC (0.23 mmol), DMAP (0.21 mmol) and HOBT (0.21 mmol) were added. The mixture was stirred at room temperature for 12 h .Upon completion, the reaction mixture was diluted with EtOAc and washed with water (3 × 30 mL). The organic phase was dried over Na_2SO_4 and concentrated under reduced pressure. The crude product was purified by silica gel chromatography using methanol/dichloromethane (v/v, 1:25) to give compound **8** as solid. ^{1}H NMR (400 MHz, $CDCl_3$) δ 7.82 – 7.77 (m, 6H), 7.74 – 7.71 (m, 3H), 7.66 – 7.62 (m, 6H), 5.64 (d, J = 9.9 Hz, 1H), 5.35 (s, 1H), 3.99 – 3.82 (m, 2H), 3.01 – 2.93 (m, 1H), 2.76 – 2.71 (m, 1H), 2.47 – 2.44 (m, 1H), 2.32 – 2.35 (m, 1H), 1.95 – 1.81 (m, 4H), 1.69 – 1.62 (m, 2H), 1.56 – 1.53 (m, 2H), 1.30 – 1.18 (m, 7H), 0.89 (d, J = 5.8 Hz, 3H), 0.77 (d, J = 7.1 Hz, 3H). ^{13}C NMR (100 MHz, $CDCl_3$) δ 171.87, 135.04, 133.76, 130.52, 118.56, 117.70, 104.43, 92.25, 91.86, 80.10, 51.51, 45.16, 37.29, 36.17, 34.04, 31.56, 25.85, 24.57, 21.98, 20.23, 17.96, 12.22. ESI $[M-Br]^+$ m/z calcd. for [C37H44O6P] 615.29, found 615.28 $[M-Br]^+$.

2.2 Kinetic study of the reaction between the synthetic Bobpy (4) and •OH

Coumarin-3-carboxylic acid (Coumarin-CA) is a commercially available and well-studied fluorescence probe for ·OH detection. Herein, it was chosen for comparison with compound **4**. The reaction between ·OH and Coumarin-CA will generate a fluorescent product 7-hydroxycoumarin-3-carboxylic acid with blue light emission peaked at 454 nm under 400 nm excitation. Therefore, monitoring this reaction is approachable by checking the fluorescence intensity I_{454}. Meanwhile, we found that ·OH reacting with compound **4** can decrease its UV-vis absorbance peaked at 610 nm, thus offering a simple way to monitor the reaction. In a typical test, Coumarin-CA (100 μM) or compound **4** (40 μM) were incubated with Fenton reagent EDTA-Fe^{2+} (100 μM) and H_2O_2 (10 mM) in sodium borate buffer (pH 9.0). For a competition experiment, both Coumarin-CA and compound **4** were mixed for test. The mixture was prepared in a 96-well plate, emission intensity I_{454} under 400 excitation and UV-vis absorbance intensity I_{610} were recorded with kinetic cycles (10-second interval). See figure S2.

2.3 Hydroxyl radical detection in aqueous solutions

Standard 1 x PBS buffer (137 mM NaCl, 10 mM phosphate, 2.7 mM KCl, pH 7.4) was used thoroughly as the aqueous medium for test. EDTA-Fe^{2+} complex was applied for Fenton reaction instead of ferrous salt, mainly because that it is a mild catalyst and has been previously used for ·OH production in aqueous mediums and in biological systems. In a typical test, Rho-Bob was mixed with EDTA-Fe^{2+} in solutions, followed by the addition of hydrogen peroxide to reach the designed final concentrations at 0, 2, 5, 10, 15, 20, 25, 50, 100 μM, respectively. The final concentrations of Rho-Bob and EDTA-Fe^{2+} were set at 20 μM and 200 μM respectively. For the measurement based on a 96-well plate, 200 μL per well reaction mixture was applied. The reaction was performed at rt for 2.5 hours before fluorescence measurement by a plate reader. Three repeats were set for each test. For the detection of ·OH induced H_2O_2 photolysis, Rho-Bob (20 μM) was mixed with H_2O_2 (10 mM) in ACN/PBS (2:1) solution. The solution was exposed to a UV light (254 nm, 5 W) for ·OH generation. To collect the fluorescence, Rho-Bob was excited at 525 nm.

Note: *Compared with Fe^{2+}/H_2O_2, Fenton reaction through EDTA- Fe^{2+}/H_2O_2 has greatly decreased reaction rate, thus making it easier to control. That is one of the reasons why chelate-Fe^{2+} complexes including EDTA- Fe^{2+} have been widely used for organic pollution degradation, through Fenton reaction.[3] Moreover, EDTA-Fe^{2+}/H_2O_2 has previously been used as a mild system to generate hydroxyl radicals in living cells.[4] In other hand, free Fe^{2+} ions are easy to form precipitates when complexed with PO_4^{3-} in buffer solutions, which will affect the test. With above consideration, we chose EDTA- Fe^{2+}/H_2O_2 to generate hydroxyl radicals.*

2.4 Living cell imaging and intracellular •OH detection

HeLa cells were maintained in DMEM basic medium plus 10% FBS and 1% (v/v) penicillin/streptomycin mix. For cell imaging, HeLa cells were seeded in the petri dishes with cover glass bottom. Rho-Bob (10 μM) was added into the culture medium and incubated for 30 min. The medium was replaced by fresh DMEM and the cells were imaged by a Leica confocal microscopy (TCS-SPE-II). The 532 nm laser was used to excite the molecule. To minimize the influences from partial overlap of emission spectra of these two fluorophores, the detection windows for Rho and Bobpy were set from 580 nm to 600 nm and from 640 nm to 660 nm, respectively. To facilitate the observation and analysis, the

fluorescence signal from Rho was marked as green, and the signal from Bobpy was marked as red. Cellular localization of Rho-Bob was checked by co-incubation with commercial Mito Tracker (Mito green) 5 μM. Pearson correlation coefficient (PCC) was used to quantitatively analyze colocalization, which was calculated using software Image J with a plugin Coloc-2 following its standard procedure [5].

For intracellular ·OH imaging, Rho-Bob (10 μM) was incubated with the cells for 30 min. The medium was then replaced with fresh DMEM followed by sequential addition of H_2O_2 (1 mM) and EDTA-Fe^{2+} (200 μM). Fluorescence images were taken every few minutes after addition of EDTA-Fe^{2+}. To image ·OH generated from drug activation, the cells were incubated with Rho-Bob (10 μM) in the presence of drugs dihydroartemisinin (DHA) or its triphenyl phosphine derivative DHA-TPP at designed concentrations. 4 hours later, the medium was replaced with fresh DMEM and the cells were observed under microscope. Quantitative analysis of images was performed using software Image J.

2.5 Ratiometric fluorescence image •OH in living zebrafishes

The protocols for use of zebrafish were approved by the Animal Ethics Committee of Guangzhou University of Chinese Medicine, in accordance with the national regulatory principles. Wild-type larval zebrafish at 3 days post fertilization were raised synchronously at 28.0 °C in embryo medium (540 μM KCl, 13.7 mM NaCl, 300 μM $CaCl_2$, 44 μM KH_2PO_4, 25 μM Na_2HPO_4, 420 μM $NaHCO_3$, 100 μM $MgSO_4$, pH 7.4). To perform *in vivo* imaging of ·OH, zebrafishes at 5 days post-fertilization (hpf) were used. To the culture medium, Rho-Bob (5 μM) was added followed by incubation at 28.0 °C for 24 hours before imaging. N-acetylcysteine (NAC) is well-described hydroxyl radical scavenger [6], which has been applied in our study to neutralize the potential ·OH in *z*ebrafish. To do this, NAC (100 μM) was incubated together with Rho-Bob (5 μM) in zebrafish cultures. After incubation, the medium was removed and the zebrafish was washed twice with PBS buffer and then fixed on a cover slip with 10% glycerol (PBS solution) containing tricane (150 μg/mL) for fish anesthesia. Zebrafish imaging was performed by the same Leica confocal microscopy under the same filter settings as done for living cell imaging. Fluorescence signal quantification was performed by Image J (see section 15).

3. Fluorescence and UV-vis absorbance properties of compound 4

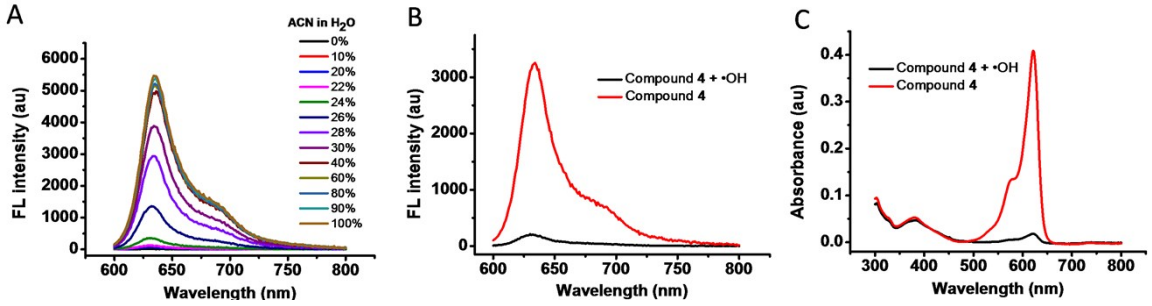

Fig. S1. A) Fluorescence spectra of compound **4** (20 μM) in different solvent mixtures (ACN/H_2O); B) fluorescence spectrum of compound **4** (20 μM) in ACN/PBS 2:1 solution in the presence and in the absence of ·OH (H_2O_2 50 μM, EDTA-Fe^{2+} 200 μM), excited at 580 nm; C) The corresponding UV-vis absorption spectra of compound **4** with or

without ·OH.

4. Reaction mechanism

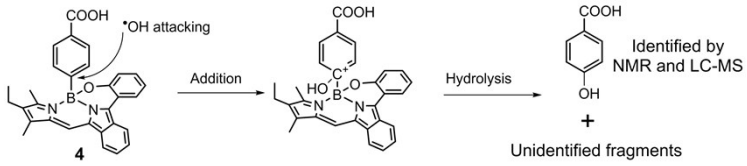

Fig. S2. Proposed mechanism of the reaction between compound **4** and ·OH

The reaction may start by the addition of ·OH to the atom 3(C). A further hydrolysis reaction occurs to generate corresponding phenol group, which has been identified by NMR and Mass spectrum. Other fragments are also nonfluorescent, but unfortunately, they failed to be structurally indentified.

Table S1. Condensed Fukui function for prediction of reactivates.

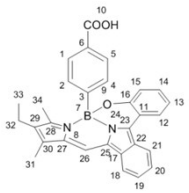

Atom	q(N)	q(N+1)	q(N-1)	f^-	f^+	f^0
1(C)	-0.0311	-0.0212	-0.0407	-0.0097	-0.0098	-0.0098
2(C)	-0.0412	-0.0418	-0.0412	-0.0001	0.0006	0.0003
3(C)	-0.0739	-0.0884	-0.0594	0.0145	0.0146	0.0145
4(C)	-0.0469	-0.0539	-0.0406	0.0064	0.007	0.0067
5(C)	-0.0494	-0.0414	-0.0575	-0.0081	-0.008	-0.008
6(C)	-0.0311	-0.0182	-0.044	-0.0129	-0.0128	-0.0129
7(B)	0.1323	0.1324	0.1281	-0.0042	-0.0001	-0.0021
8(N)	-0.0576	-0.0491	-0.0693	-0.0117	-0.0085	-0.0101
9(O)	-0.1845	-0.1734	-0.1957	-0.0112	-0.0111	-0.0112
10(C)	-0.0308	-0.0217	-0.032	-0.0011	-0.0091	-0.0051
11(C	-0.035	-0.018	-0.0587	-0.0237	-0.017	-0.0204
12(C)	-0.0568	-0.0315	-0.0796	-0.0228	-0.0253	-0.024
13(C)	-0.0299	0.0063	-0.0702	-0.0403	-0.0362	-0.0382
14(C)	-0.0559	-0.0415	-0.0744	-0.0186	-0.0144	-0.0165
15(C)	0.0949	0.1126	0.0785	-0.0164	-0.0177	-0.0171
16(C)	-0.0128	-0.0072	-0.0358	-0.023	-0.0056	-0.0143
17(C)	-0.0411	-0.0122	-0.0554	-0.0143	-0.0289	-0.0216
18(C)	-0.0354	-0.0051	-0.0785	-0.0431	-0.0304	-0.0367
19(C)	-0.0456	-0.0067	-0.0737	-0.028	-0.0389	-0.0335
20(C)	-0.0338	-0.0081	-0.0581	-0.0243	-0.0258	-0.025
21(C)	-0.0236	-0.0086	-0.0372	-0.0135	-0.0151	-0.0143
22(C)	0.0782	0.1193	0.0087	-0.0694	-0.0411	-0.0553
23(N)	-0.03	-0.0318	-0.0573	-0.0273	0.0019	-0.0127

24(C)	0.0086	0.0807	0.0026	-0.0059	-0.0722	-0.039
25(C)	-0.0095	-0.0034	-0.0956	-0.0861	-0.0062	-0.0461
26(C)	-0.0002	0.0705	-0.0076	-0.0074	-0.0707	-0.039
27(C)	0.0657	0.13	0.0187	-0.047	-0.0643	-0.0556
28(C)	-0.0429	0.0017	-0.0673	-0.0244	-0.0446	-0.0345
29(C)	-0.0157	0.0106	-0.0584	-0.0427	-0.0263	-0.0345
30(C)	-0.0804	-0.0695	-0.0922	-0.0118	-0.0108	-0.0113
31(C)	-0.0473	-0.039	-0.0529	-0.0057	-0.0082	-0.0069
32(C)	-0.0869	-0.0767	-0.094	-0.0071	-0.0102	-0.0087
33(C)	-0.0809	-0.0652	-0.0936	-0.0128	-0.0156	-0.0142
34(C)	0.2045	0.2088	0.1994	-0.0051	-0.0043	-0.0047
35(O)	-0.2684	-0.2515	-0.2858	-0.0174	-0.0169	-0.0171
36(O)	-0.1932	-0.1825	-0.2039	-0.0108	-0.0106	-0.0107

Note: FREQ calculation was performed by Gaussian 09. Density functional theory (DFT) based basis set: G-311G(d), method: RM062X, Spin: Singlet. Both Gaussian and the software Multifwn (multifunctional wave-function analysis) were used for analysis [7]. The condensed Fukui functions were calculated using the Hirshfeld charge.

The Fukui function for prediction of radical attacking can be described as

$$f^0 = \frac{f^+ + f^-}{2} = \frac{q(N+1) - q(N-1)}{2} \qquad \text{Equation S1}$$

For the Fukui function, the region with a larger positive value is more likely to be attacked by free radicals [8]. f^0 of all the atoms in compound **4** except hydrogen have been listed in Table S1. As shown in Table S1, the atom 3(C) exhibits the largest positive value, which indicating the greatest reactivity toward hydroxyl radicals.

In the calculation, condensed Fukui function (Equation S1) was used to describe local chemical reactivity toward free radicals. As shown in Table S1, the atom 3 (C) in C-B bond exhibits the largest positive value, which indicating the greatest reactivity toward ·OH.[9] The theoretical found out is consisted with the experimental observation.

5. Kinetic competition study

The kinetics of the reaction between compound **4** and ·OH could be monitored by measuring changes of UV-vis absorbance at 610 nm. On the other hand, ·OH reacting on Coumarin-CA will generate a fluorescent product 7-hydroxycoumarin-3-carboxylic acid, which could be monitored by the increases of emission intensity I_{454} under 400 nm excitation. As indicated from Fig. S3, the time course kinetics analysis shows an obvious increase of I_{454} when Coumarin-CA was incubated with Fenton reagents in the absence of compound **4**. Nevertheless, the generation of fluorescence product was greatly reduced when Coumarin-CA and compound **4** were co-incubated with the Fenton reagents. In contrast, Coumarin-CA co-incubation did not lead to significant influence to the reaction rate between compound **4** and ·OH.

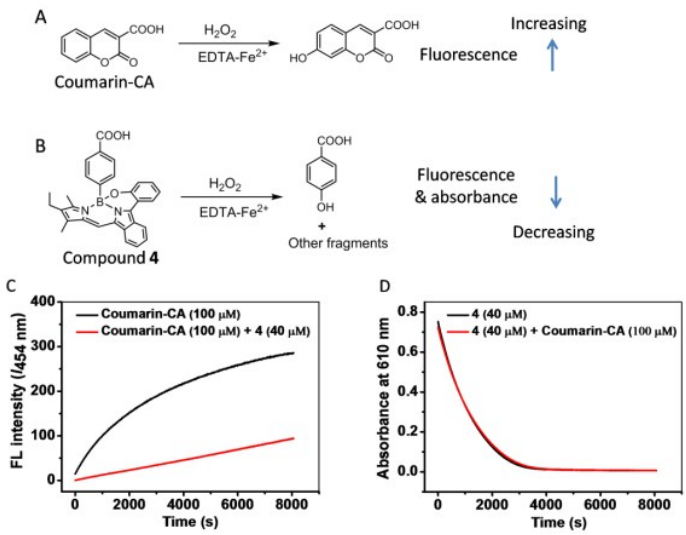

Fig. S3. (A) ·OH reaction on the commercial Coumarin-CA generates a fluorescent product; (B) synthetic compound **4** decomposes to non fluorescence fragments upon ·OH attacking; (C) Kinetic study of the reaction between ·OH and Coumarin-CA monitored by fluorescence intensity measurement (I_{454} under 400 nm excitation) in the presence and in the absence of compound **4**; (D) Kinetic study of the reaction between ·OH and compound **4** through measurement of UV-vis absorbance at 610 nm, in the presence and in the absence of Coumarin-CA.

6. Quantum yield and FRET efficiency calculation

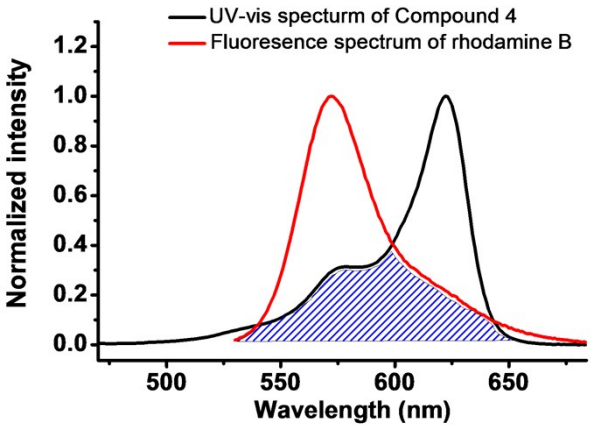

Fig. S4. The UV-vis spectrum of compound **4** and the fluorescence spectrum of rhodamine B (excited at 510 nm). The maximum intensity in both spectra has been normalized to 1.

Table S2: Relative quantum yields of rhodamine B alone and rhodamine B in the presence of FRET acceptor.

Probes	Abs（λ=510）	Area	*n*	φ
Rhodamine B	0.347	2.35E+05	1.36	0.65
Rho-Bob	0.171	1796.40	1.36	0.010

Note: the area from Rho-Bob stands for the integrated emission peak area from rhodamine B moiety only.

Table S3: Relative quantum yield of compound **4**.

Probes	Abs（λ=565）	Area	*n*	φ
Cresyl violet	0.145	1.20E+05	1.36	0.58
Compound 4	0.098	1.06E+05	1.36	0.76

The relative quantum yields of rhodamine moiety in Rho-Bob and compound **4** were measured, individually. All compounds were dissolved in ethanol at 20 μM. The quantum yields of rhodamine B (φ =0.65 in ethanol) [10] and cresyl violet (φ =0.58 in ethanol) [11] were set as references for Rho-Bob and for compound **4** respectively. The relative quantum yields were calculated by the following equation [12].

$$\varphi_S = (Abs_R/Abs_S)\times(Area_S/Area_R) \times(n_S/n_R) \times\varphi_R \qquad \text{Equation S2}$$

where the subscripts R and S refer to the reference and samples respectively. Abs, Area and *n* are the absorbance at the excitation wavelength (510 nm for both rhodamine B and Rho-Bob; 565 nm for cresyl violet and compound **4**), area under the fluorescence spectrum and refractive index of the solvent respectively. Refractive index (*n*) of pure ethanol at room temperature is 1.36.

FRET efficiency (E) has been calculated using steady state fluorescence data by the following equation:

$$E = (1 - \varphi DA/\varphi D) \times 100\% \qquad \text{Equation S3}$$

φDA = Donor (rhodamine B) quantum yield in the presence of acceptor, φD = Donor alone quantum yield.

Thus, E = (1-0.010/0.65) ×100% = 98.5%

Theoretically, E can be calculated according to:

$$E = \frac{1}{1 + (R/R_0)^6} \qquad R_0 = 0.2108\left[n^{-4}\phi_d\kappa^2 J\right]^{1/6} \qquad \text{Equation S4}$$

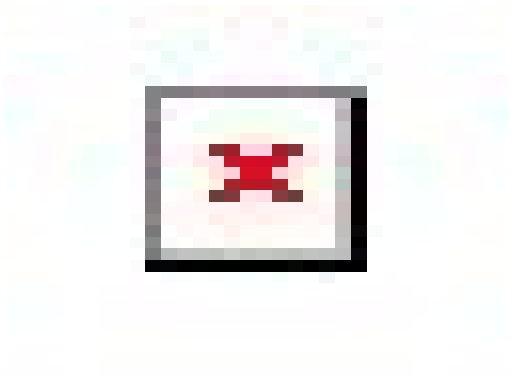

Fig. S5. Theoretic calculation estimated the distance (R) between these two fluorophores. (The molecular geometry optimization was performed by MMFF94 based energy minimization using the software SYBYL-X-2.2.1.)

The Software PhotoChemCAD 2.1 was used for this calculation on the basis of absorption spectrum of compound **4** and FL spectrum of rhodamine B. The distance between these two fluorophores in Rho-Bob was estimated to be 9.6 Å from Fig. S5. The refractive index of ethanol is n =1.36, for a random orientation k^2 is 2/3, donor's lifetime is 2.72 ns [13],

molar absorption coefficient of acceptor (45850 $M^{-1}cm^{-1}$) and donor's quantum yield (0.65, Table S1) were experimentally measured. Other parameters are adapted from the database of the software. Based on the result from PhotoChemCAD, Förster distance R_0 is found to be 52.09 Å, transfer efficiency *E* was calculated to be 99.996%.

7. Detection limits calculation

The lowest limit of detection (LOD) for ·OH in ACN/PBS (1:9) solution is estimated by a well established method (S/N=3)[14]. Briefly,

$$LOD = 3\sigma/B \qquad \text{Equation S5}$$

where σ is the standard deviation obtained from three individual measured fluorescence intensity I_{590} in the absence of ·OH. *B* is the slope from the linear fitting of the titration curve.

8. Identification of the products from Rho-Bob /·OH reaction

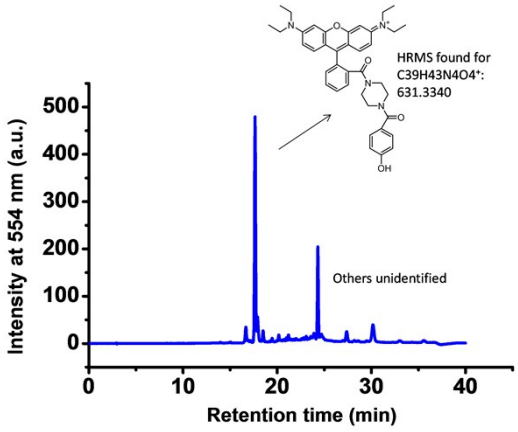

Fig. S6. HPLC and HRMS analysis of the reaction products from Rho-Bob.

9. Detection ·OH from H_2O_2 UV lysis

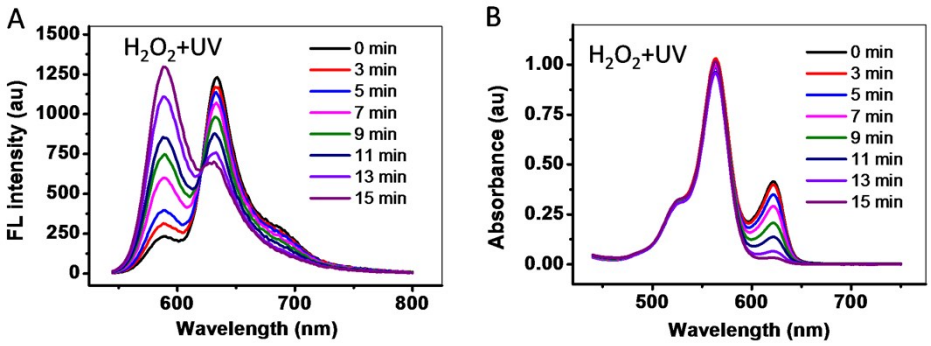

Fig. S7. A) Ratiometric fluorescence sensing of ·OH generated from H_2O_2 (10 mM) photolysis in ACN/PBS 2:1 solution; B) The corresponding UV-vis absorbance changes of Rho-Bob upon reaction with ·OH in ACN/PBS 2:1 solution.

10. Selectivity and pH effect

The anions NO_2^-, HSO_4^- and $H_2PO_4^-$, all at 500 μM were added directly from corresponding mother solutions containing $NaNO_2$, $NaHSO_4$ and NaH_2PO_4 respectively. H_2O_2 and *tert*-Butyl hydroperoxide (TBHP) solutions were added directly into the reaction mixture to reach to 500 μM, respectively. Superoxide anion $O_2^{\bullet-}$ and $ONOO^-$ were prepared using previously reported methods [15]. The concentrations were estimated to be 500 μM. The reaction mixture was kept at room temperature for 2.5 h before fluorescence measurement by a plate reader. Three repeats were set for each test. DMSO, a widely used and specific ·OH quenching reagent, was added into the detection system to further confirm the selectivity. As expected, DMSO at 5% final concentration decreased the fluorescence intensity largely in ·OH detection system, mostly because excess amount of DMSO greatly competed with Rho-Bob in ·OH reaction.

Rho-Bob weakly responds to Fe^{2+}, this is mostly because of auto-oxidation of Fe^{2+} in PBS buffers that generates ·OH. It has been reported that the phosphate complexes of Fe^{2+} will undergo fast auto-oxidation by the air, which leads to ·OH generation (Radiat Res. 1997, 148:181-7).

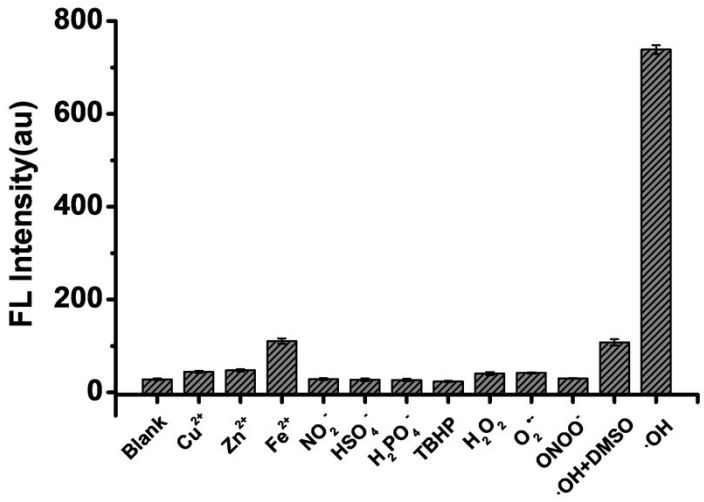

Fig. S8. Selectivity study of Rho-Bob toward ·OH detection. Rho-Bob at 20 μM in ACN/PBS 1:9 solution was used for test, biorelevant cations Cu^{2+}, Zn^{2+}, Fe^{2+}, anions NO_2^-, HSO_4^-, $H_2PO_4^-$ and some other reactive oxygen and reactive nitrogen species TBHP, H_2O_2, $O_2^{\bullet-}$, $ONOO^-$ were tested all at 500 μM, 10 folds higher than ·OH (50 μM). DMSO was used at 5% to quench ·OH.

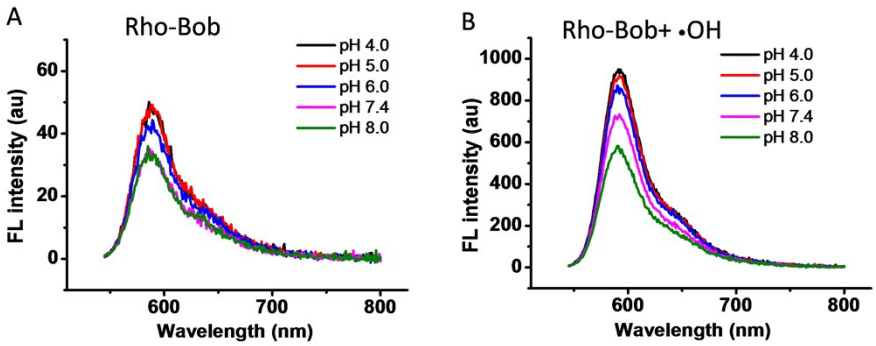

Fig. S9. pH effects on the fluorescence intensity of Rho-Bob (20 μM) in the buffer of ACN/PBS 1:9 before and after reaction with ·OH (50 μM).

11. Ratiometric imaging of ·OH in situ generated by Fenton reaction in living cells

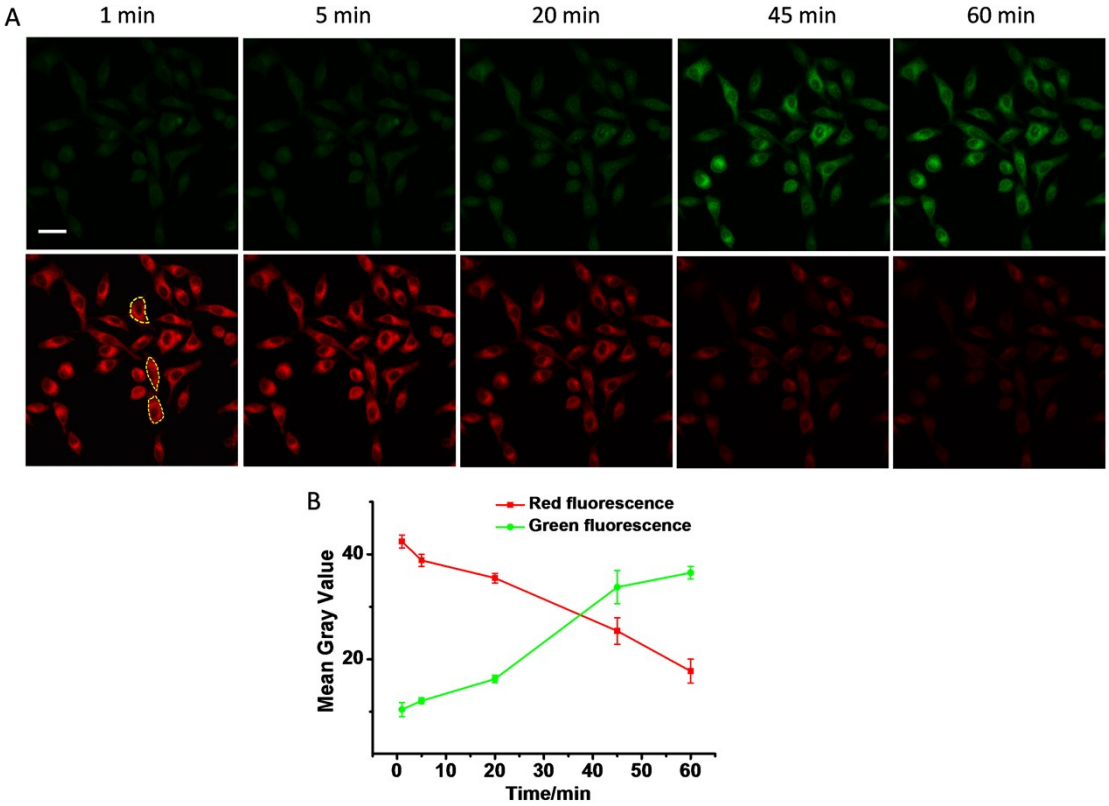

Fig. S10. A) Ratiometric fluorescence imaging of ·OH in living cells. ·OH was produced from EDTA-Fe^{2+} (200 μM)/H_2O_2 (1 mM), Rho-Bob was used at 10 μM. The images were taken at every few minutes after addition of Fenton reagents. B) Kinetic measurements of fluorescence intensity. Quantitative analysis was performed using Image J, the mean gray intensity of the selected cells (yellow color) was presented. Scale bar stands for 25 μm.

Fluorescence images were taken with time-lapse sequences, where the fluorescence from Rho is marked as green and the fluorescence from Bobpy is marked as red. In the beginning, there is an obvious red emission found in cells and the green fluorescence is very weak, which indicates that FRET occurs between Rho and Bobpy.

12. Fluorescence imaging drug activation in living cells.

Live cell imaging was performed according to the procedure described above (section 2.4). Quantitative analysis was conducted by using Image J. The figure was open with Image J. "polygon selection" was used for the selection of interested areas, this selection was then set as ROI (region of interest). For comparison study, the same region in different channels has been selected by ROI, separately. The fluorescence intensity was transferred to gray values for quantitative analysis.

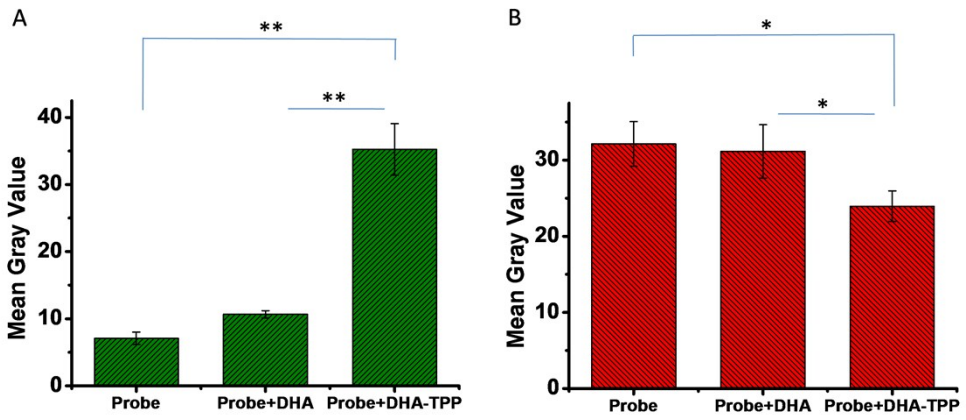

Fig. S11. Quantitatively analyze fluorescence intensity from the cells with different treatments. The data was adapted from Fig. 3 in the manuscript. Paired t-test was performed by Microsoft office excel 2007, significance level refers to significant as $P < 0.05$ (*) and highly significant as $P < 0.01$(**).

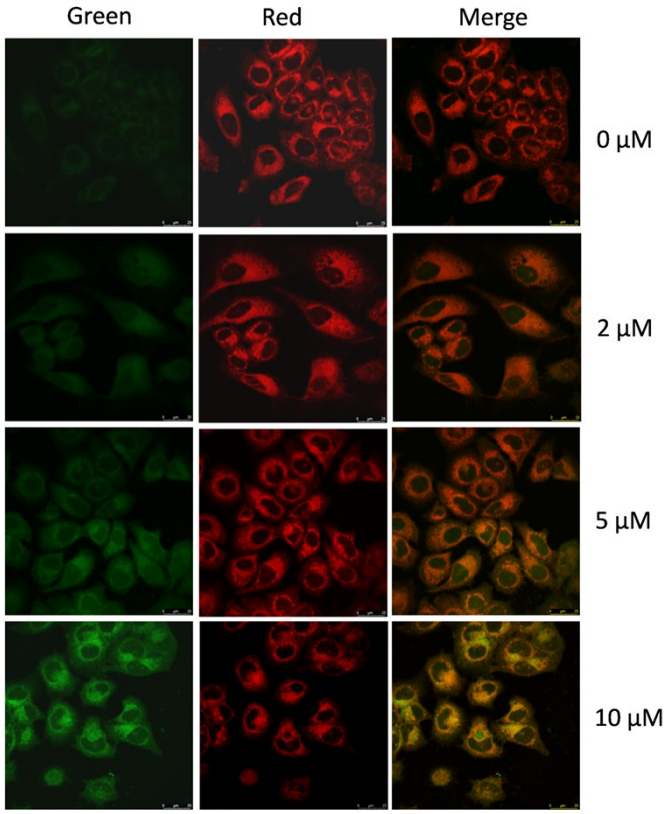

Fig. S12. HeLa cells were incubated with Rho-Bob (10 μM) in the presence of DHA-TPP at different concentrations (0, 2, 5, 10 μM). 4 hours later, the cells were imaged by a confocal microscopy.

Fig.S12 indicated that higher concentration of DHA-TPP induced more hydroxyl radicals.

13. Cell toxicity evaluation of DHA and DHA-TPP

HeLa cells were cultured at the density of 6000 cells/well in 96-well plates for 24 h. The culture medium was then

changed to fresh DMEM with various concentrations of DHA and DHA-TPP. After 72 h incubation, the medium was replaced with fresh RPMI-1640 (phenol red free) containing cell viability testing reagent resazurin (70 μM), the plate was then incubated for 2 h at 37°C. The increased UV-vis absorption at 570 nm was measured by using a Varioskan LUX plate reader (Thermo Fisher) supplied with Software SkanIt 4.1. The wells without cells but with resazurin were set as blank. Cell viability was calculated as the percentage against the cells without DHA and DHA-TPP (100%).

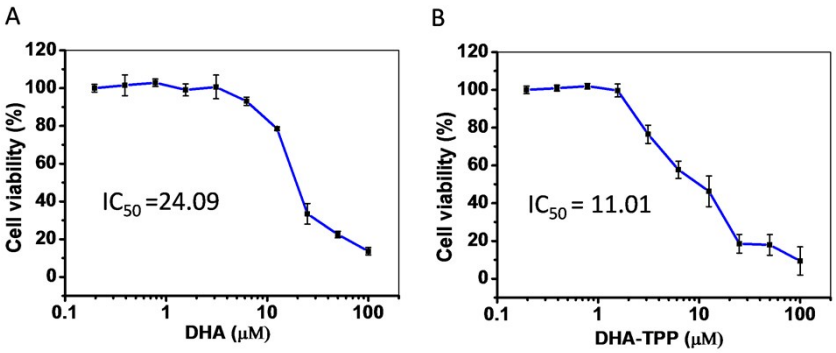

Fig. S13. Cell toxicity test of DHA and DHA-TPP. HeLa cells were incubated with the tested compound for 72 hours before cell viability evaluation by resazurin based methods.

14. Cell toxicity evaluation of Rho-Bob

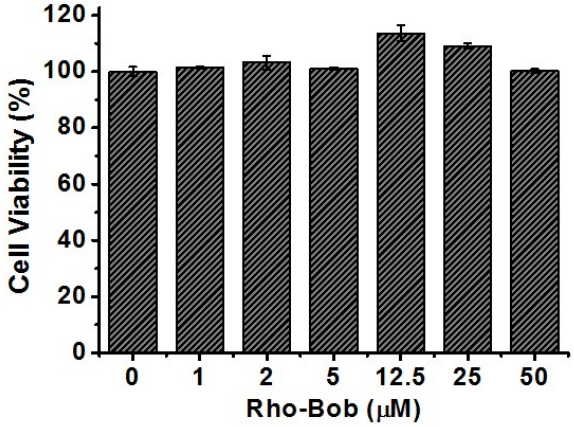

Fig. S14. Cell toxicity test of Rho-Bob. HeLa cells were incubated with Rho-Bob at different concentrations for 24 h before cell viability evaluation. Cell toxicity evaluation of Rho-Bob follows the same procedure described above.

15. Zebrafish images

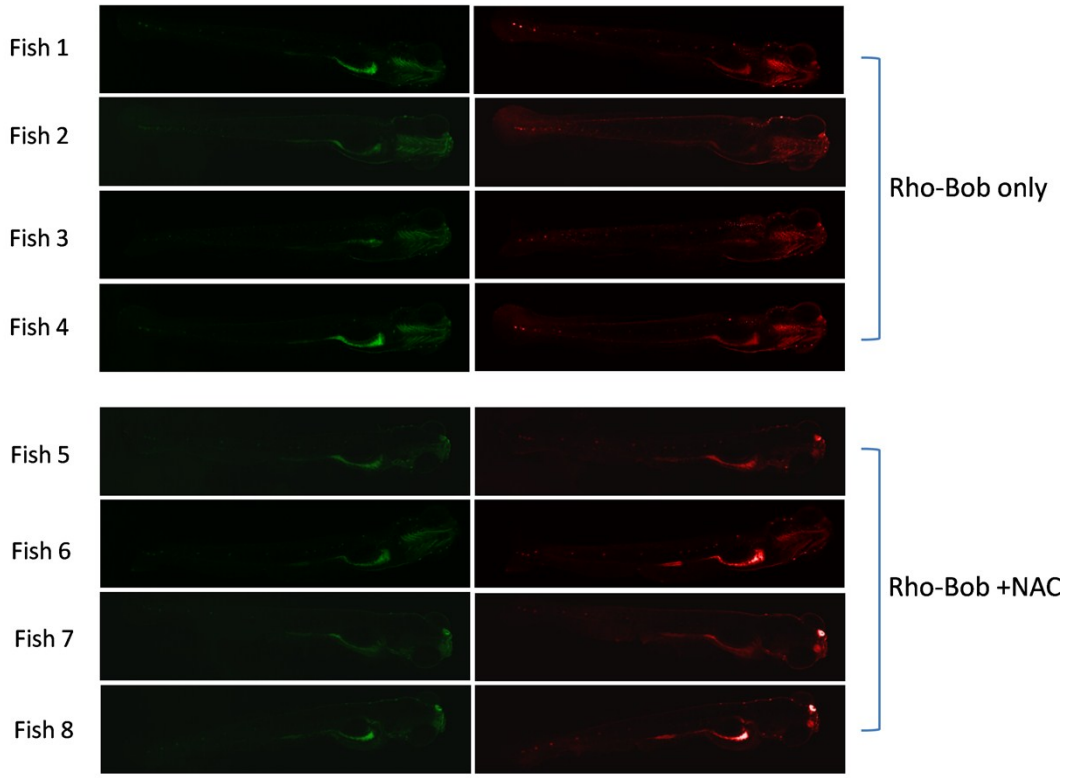

Fig. S15. Ratiometric fluorescence imaging of endogenous ·OH. Fish 1 to fish 4 were treated with Rho-Bob only, fish 5 to fish 8 were treated with Rho-Bob and NAC.

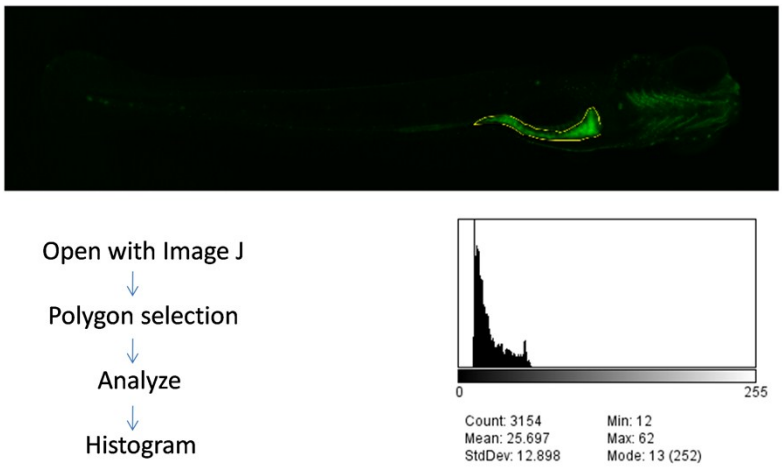

Fig. S16. The procedure for quantitative analysis of fluorescence images using Image J.

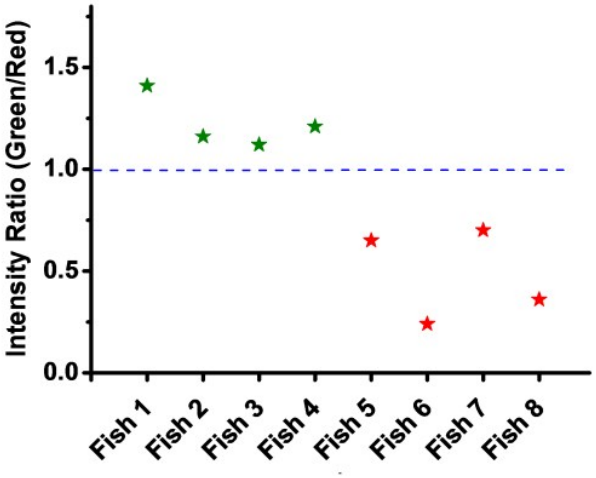

Fig. S17. Quantitative analysis of fluorescence intensity from zebrafish images. The ratio of mean intensity (green to red) from the GI tracts of zebrafish was presented. Fish 1 to fish 4 were treated with Rho-Bob only, Fish 5 to fish 8 were treated with both Rho-Bob and NAC.

16. References

1. N. Chen, W. Zhang, S. Chen, Q. Wu, C. Yu, Y. Wei, Y. Xu, E. Hao and L. Jiao, *Org. Lett.*, 2017, **19**, 2026-2029.
2. V. Bala, S. Jangir, D. Mandalapu, S. Gupta, Y. S. Chhonker, N. Lal, B. Kushwaha, H. Chandasana, S. Krishna, K. Rawat, J. P. Maikhuri, R. S. Bhatta, M. I. Siddiqi, R. Tripathi, G. Gupta and V. L. Sharma, *Bioorg. Med. Chem. Lett*, 2015, **25**, 881-886.
3. J. Ma, W. Ma, W. Song, C. Chen, Y. Tang, J. Zhao, Y. Huang, Y. Xu and L. Zang, *Environ. Sci. Technol.*, 2006, **40**, 618-624.
4. B.-Z. Zhu, L. Mao, C.-H. Huang, H. Qin, R.-M. Fan, B. Kalyanaraman and J.-G. Zhu, *Proc. Natl. Acad. Sci.*, 2012, **109**, 16046-16051.
5. S. Bolte and F. P. Cordelieres, *J Microsc*, 2006, **224**, 213-232.
6. Y. Pei, H. Liu, Y. Yang, Y. Yang, Y. Jiao, F. R. Tay and J. Chen, *Oxidative med. cell. longev.*, 2018, **2018**, 14.
7. T. Lu and F. Chen, *J. Comput. Chem.*, 2012, **33**, 580-592.
8. T. Luo, J. Wan, Y. Ma, Y. Wang and Y. Wan, *Environmental Science: Processes & Impacts*, 2019, **21**, 1560-1569.
9. T. Luo, J. Wan, Y. Ma, Y. Wang and Y. Wan, *Environ Sci. Process Impacts*, 2019, **21**, 1560-1569.
10. R. F. Kubin and A. N. Fletcher, *J. Lumin.*, 1982, **27**, 455-462.
11. A. Alessi, M. Salvalaggio and G. Ruzzon, *J. Lumin.*, 2013, **134**, 385-389.
12. V. S. Nair, Y. Pareek, V. Karunakaran, M. Ravikanth and A. Ajayaghosh, *Phys. Chem. Chem. Phys.*, 2014, **16**, 10149-10156.
13. A. S. Kristoffersen, S. R. Erga, B. Hamre and Ø. Frette, *J. Fluoresc.*, 2014, **24**, 1015-1024.
14. A. Shrivastava and V. Gupta, *Chron young sci*, 2011, **2**, 21-25.
15. X. Bai, Y. Huang, M. Lu and D. Yang, *Angew. Chem. Int. Ed. Engl.*, 2017, **56**, 12873-12877.

17. Spectra

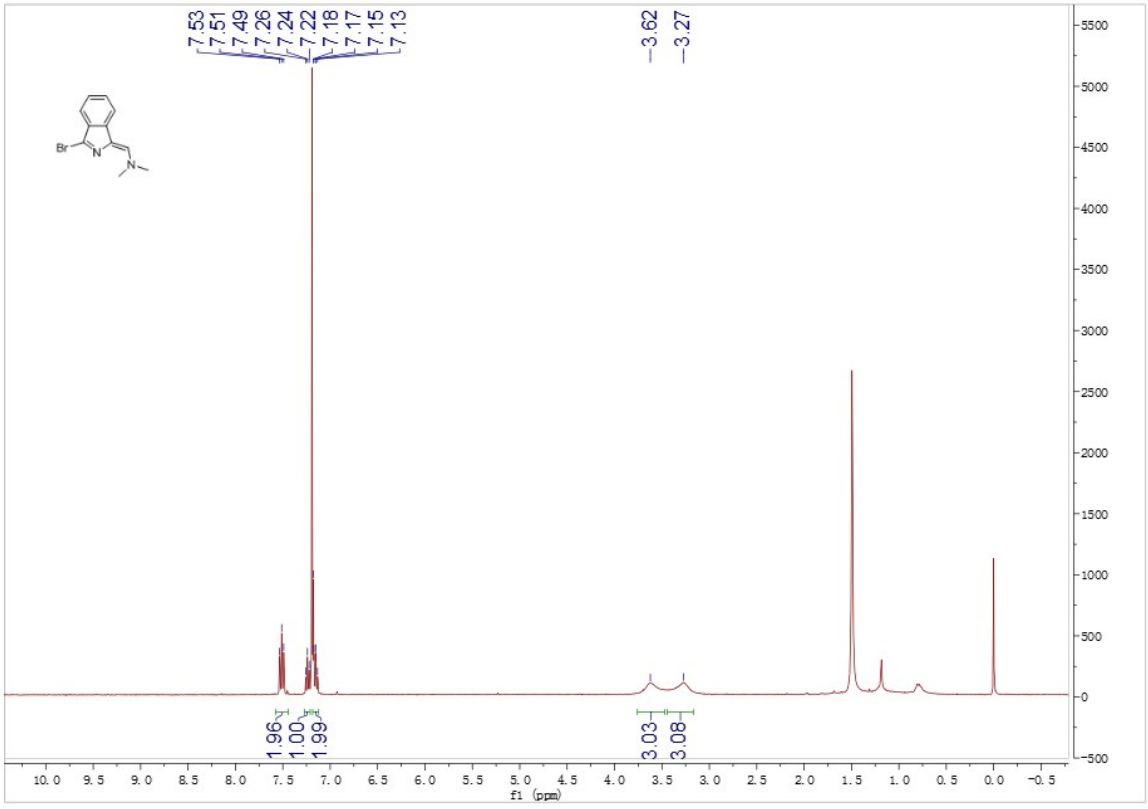

Fig. S18 ^{1}H NMR spectrum of compound **2**

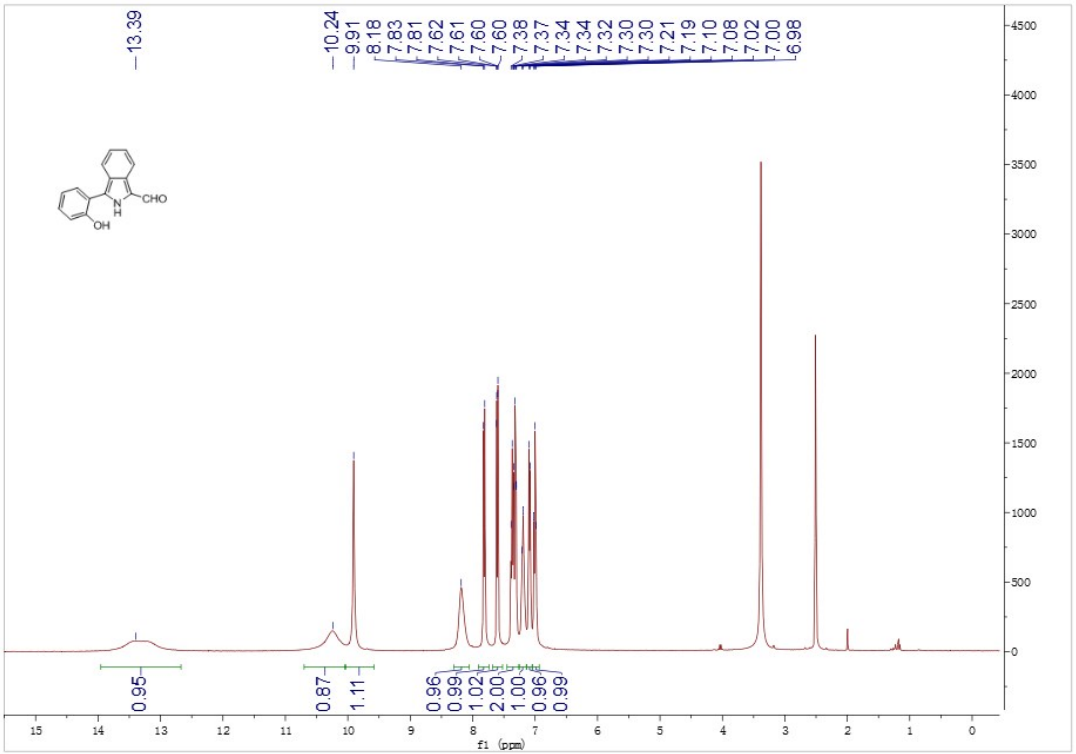

Fig. S19 ^{1}H NMR spectrum of compound **3**

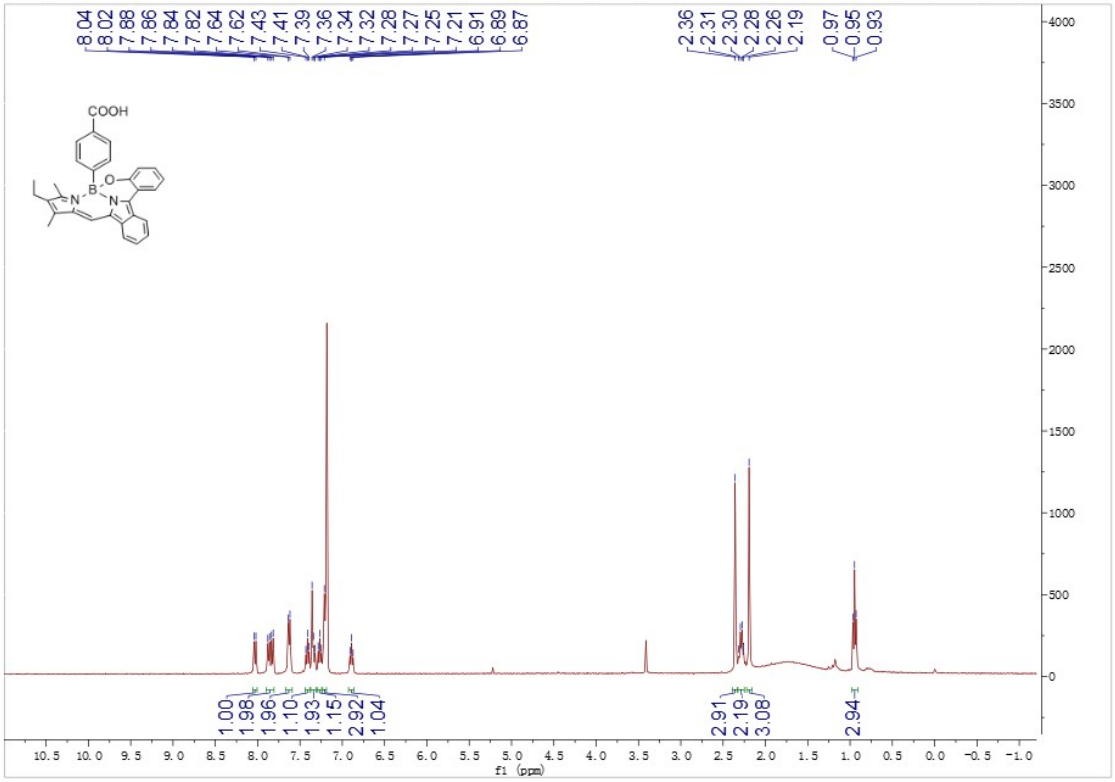

Fig. S20 ^{1}H NMR spectrum of compound **4**

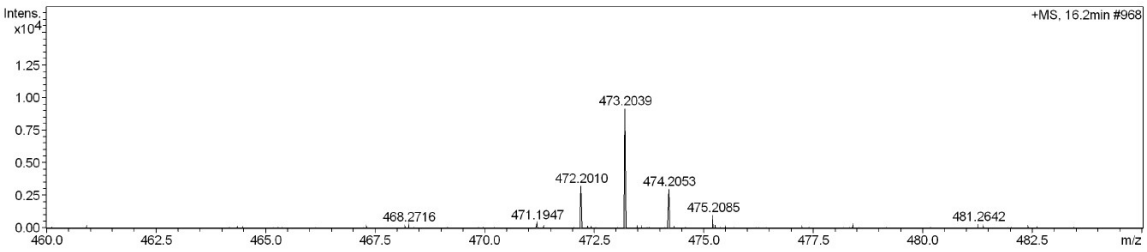

Fig. S21 HRMS spectrum of compound **4**

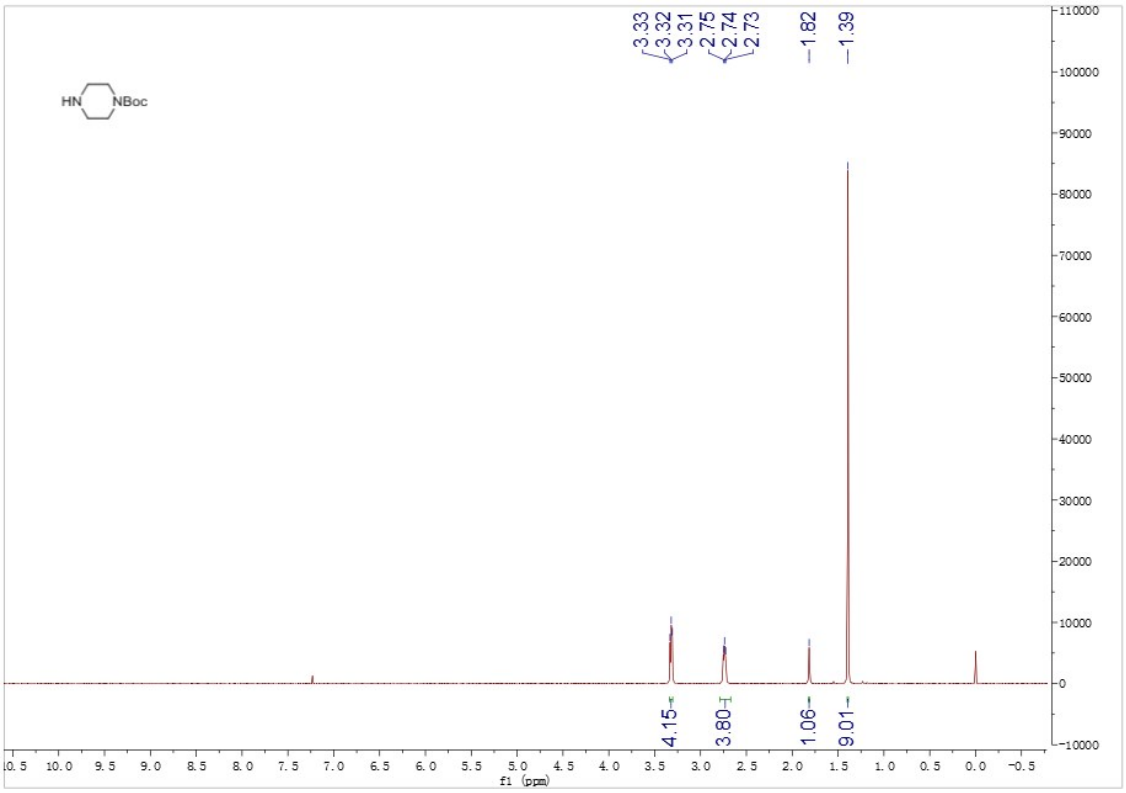

Fig. S22 ^{1}H NMR spectrum of *tert*-butyl piperazine-1-carboxylate

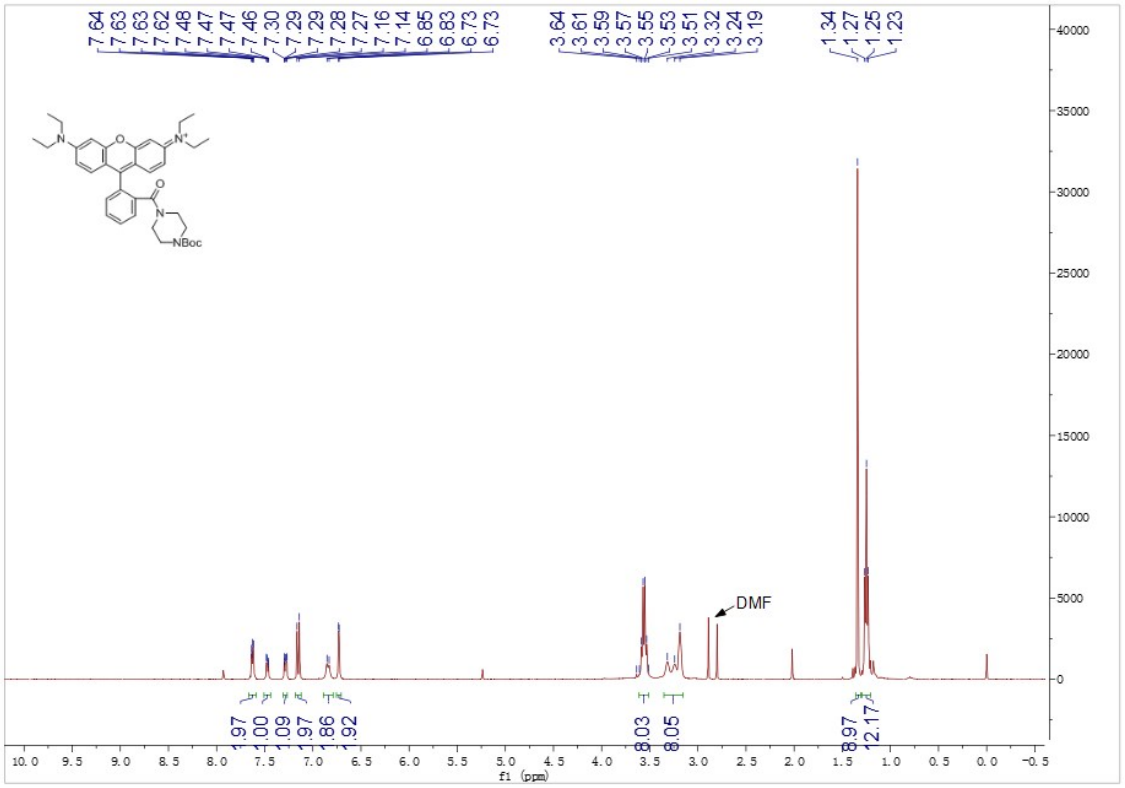

Fig. S23 ^{1}H NMR spectrum of Rhodamine-N-piperrazine-N-Boc

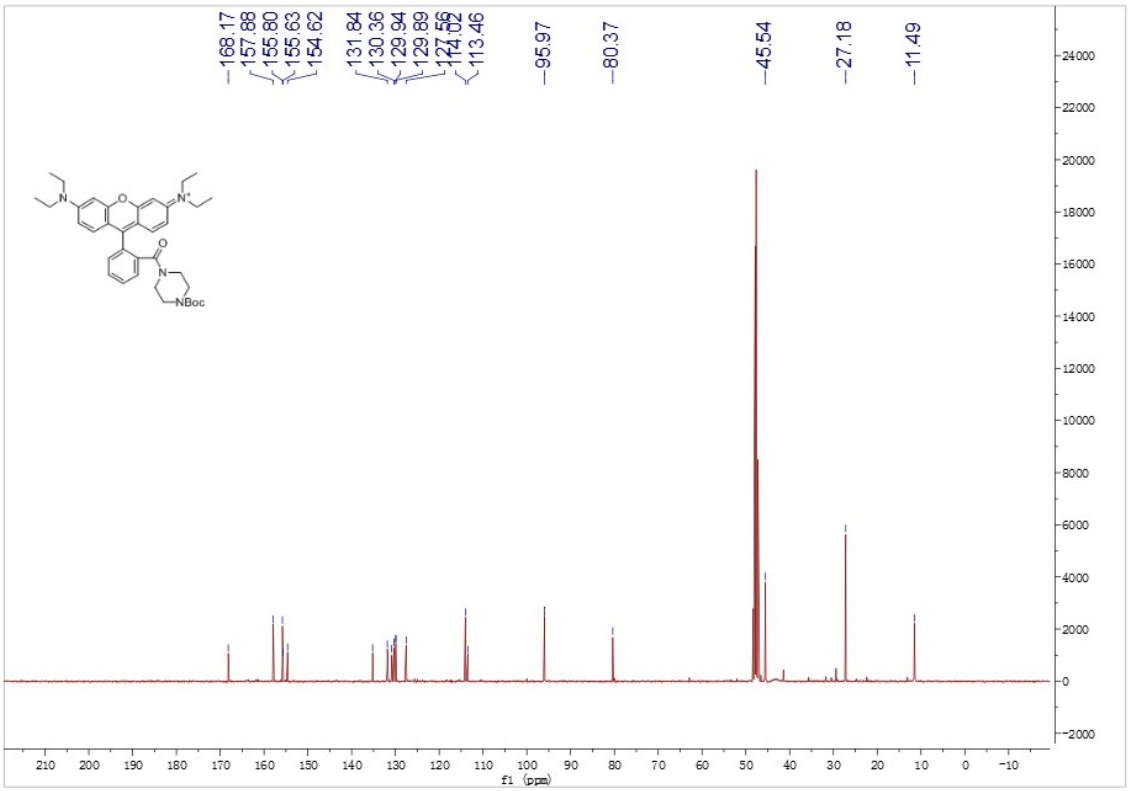

Fig. S24 ^{13}C NMR spectrum of compound **8**

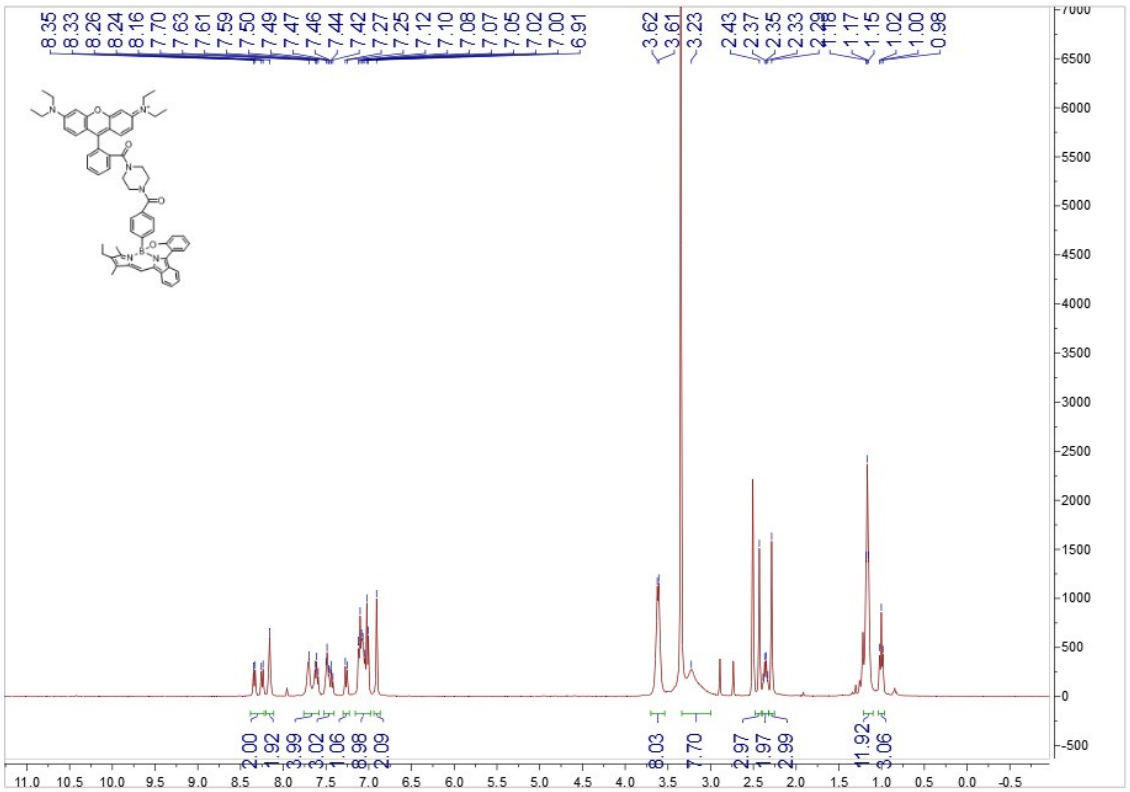

Fig. S25 ^{1}H NMR spectrum of Rho-Bob

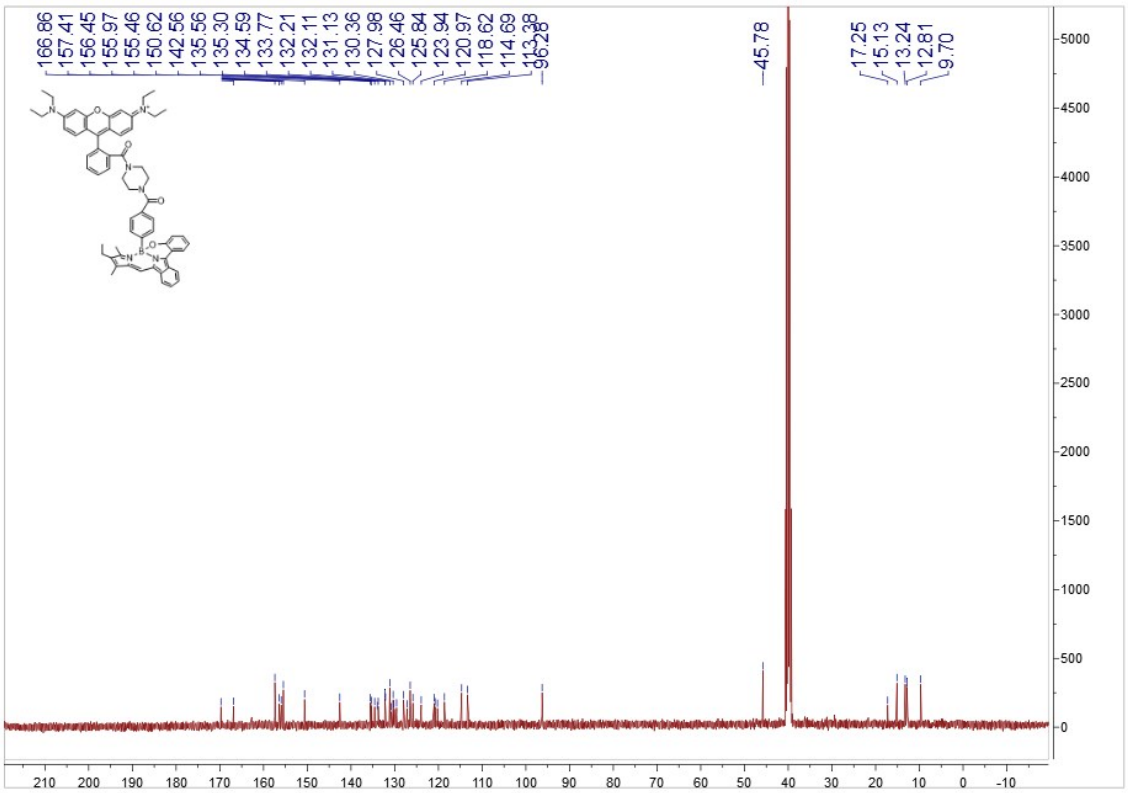

Fig. S26 ^{13}C NMR spectrum of Rho-Bob

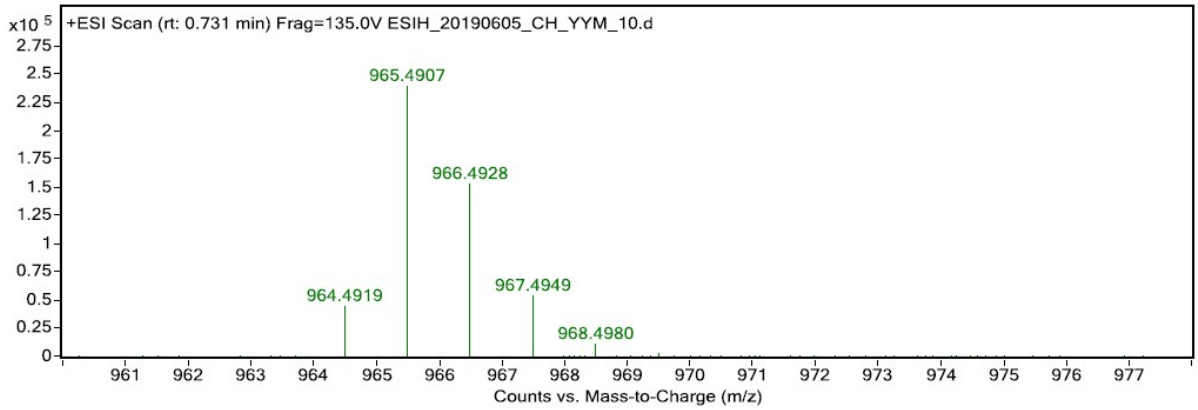

Fig. S27 HRMS spectrum of Rho-Bob

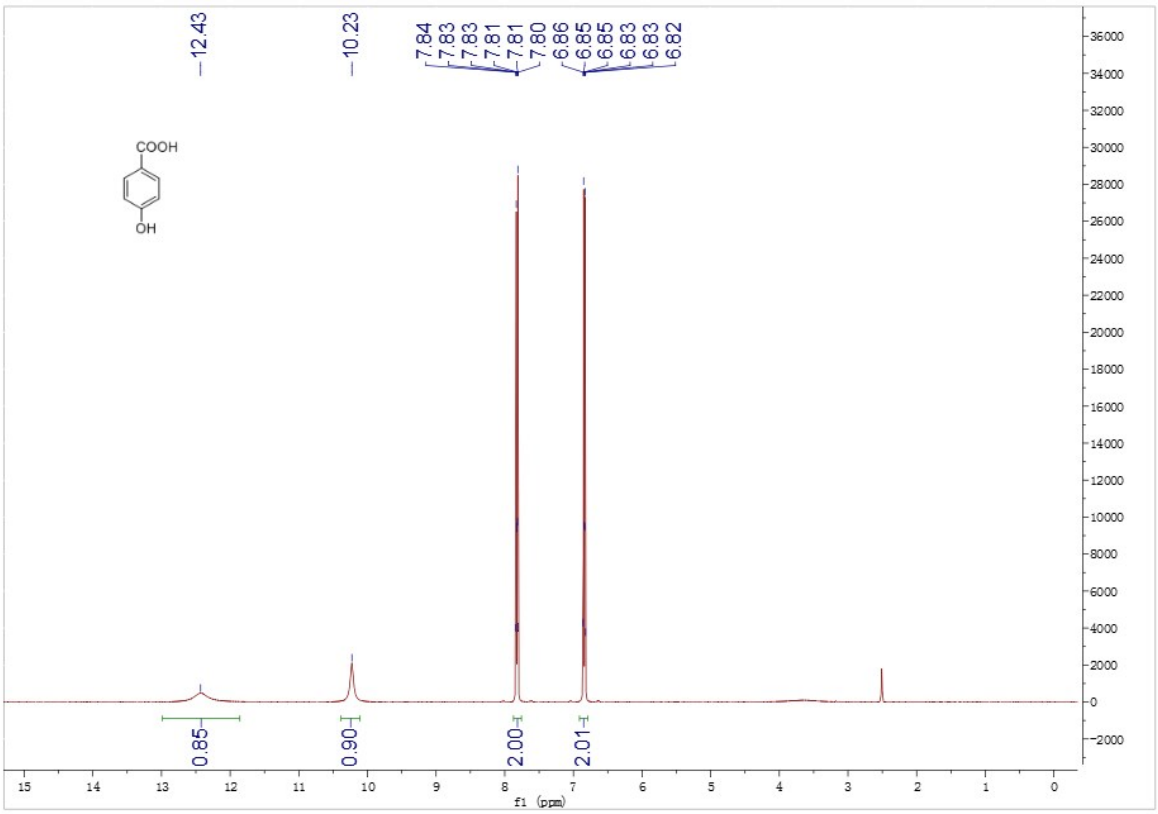

Fig. S28 ^{1}H NMR spectrum of separated product of compound **4**

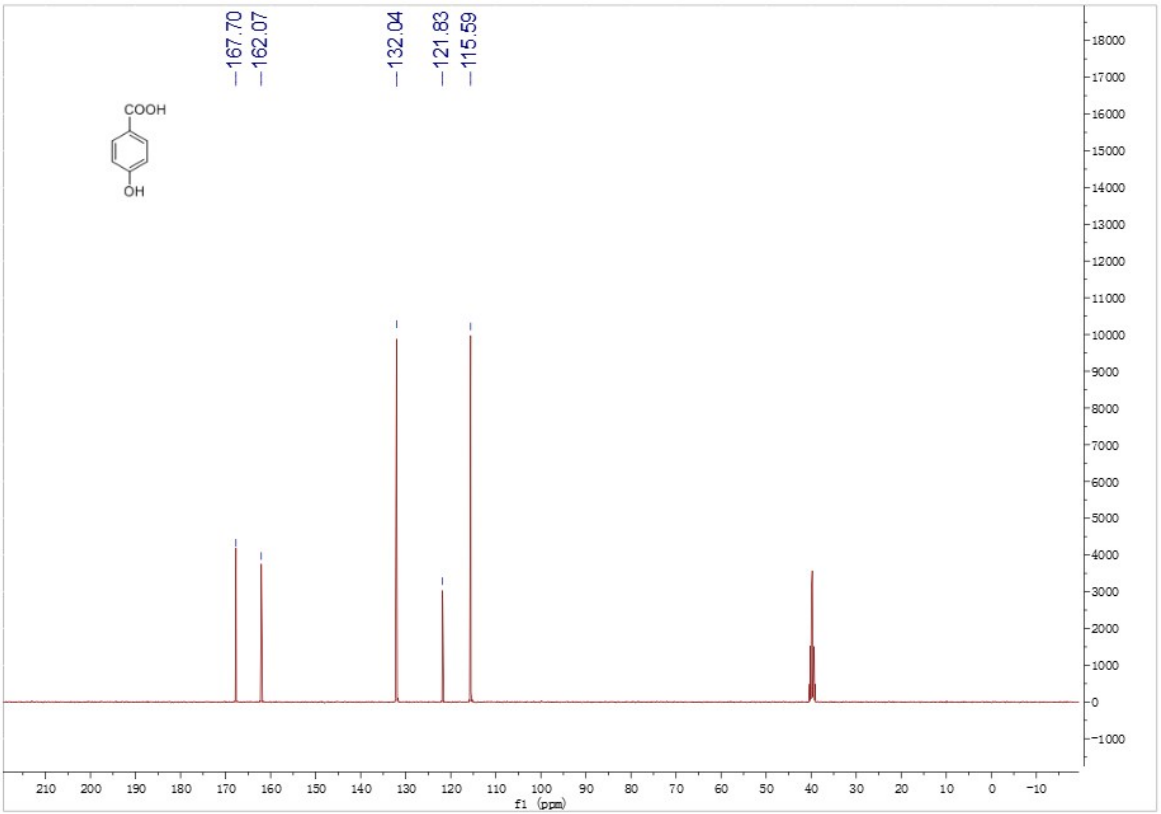

Fig. S29 ^{13}C NMR spectrum of separated product of compound **4**

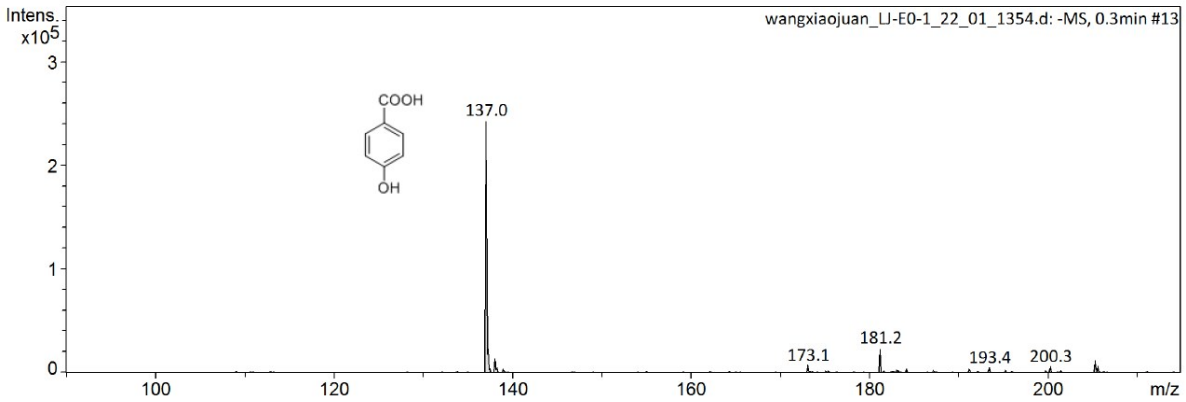

Fig. S30 Product's mass data of compound **4** after reaction with •OH

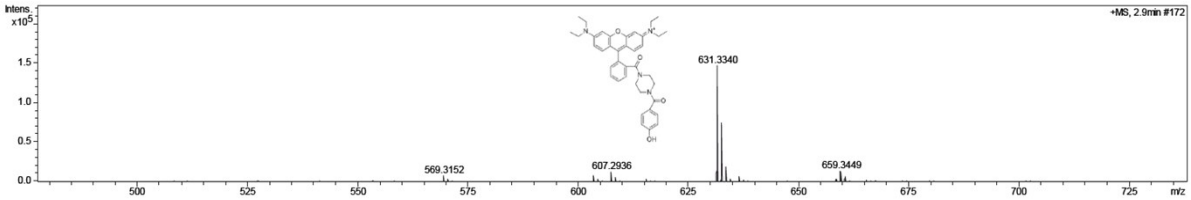

Fig. S31 HRMS data of Rho-Bob after reaction with •OH

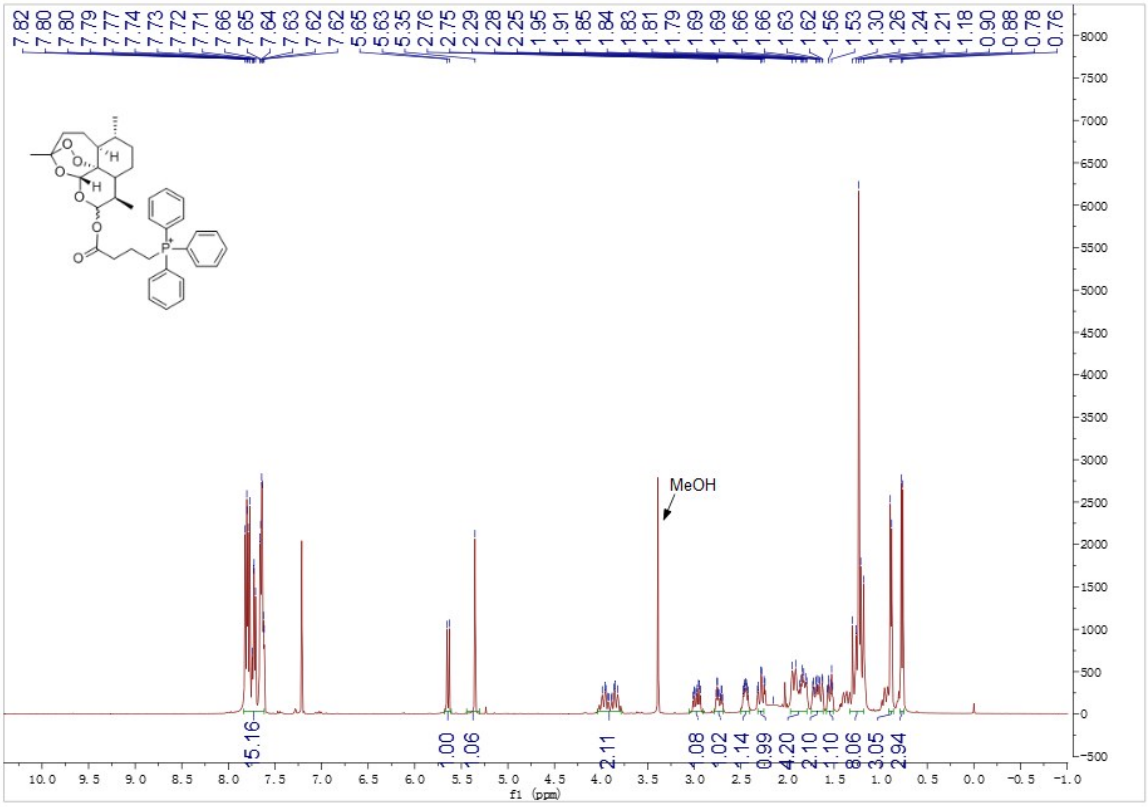

Fig. S32 ^{1}H NMR spectrum of compound **8**

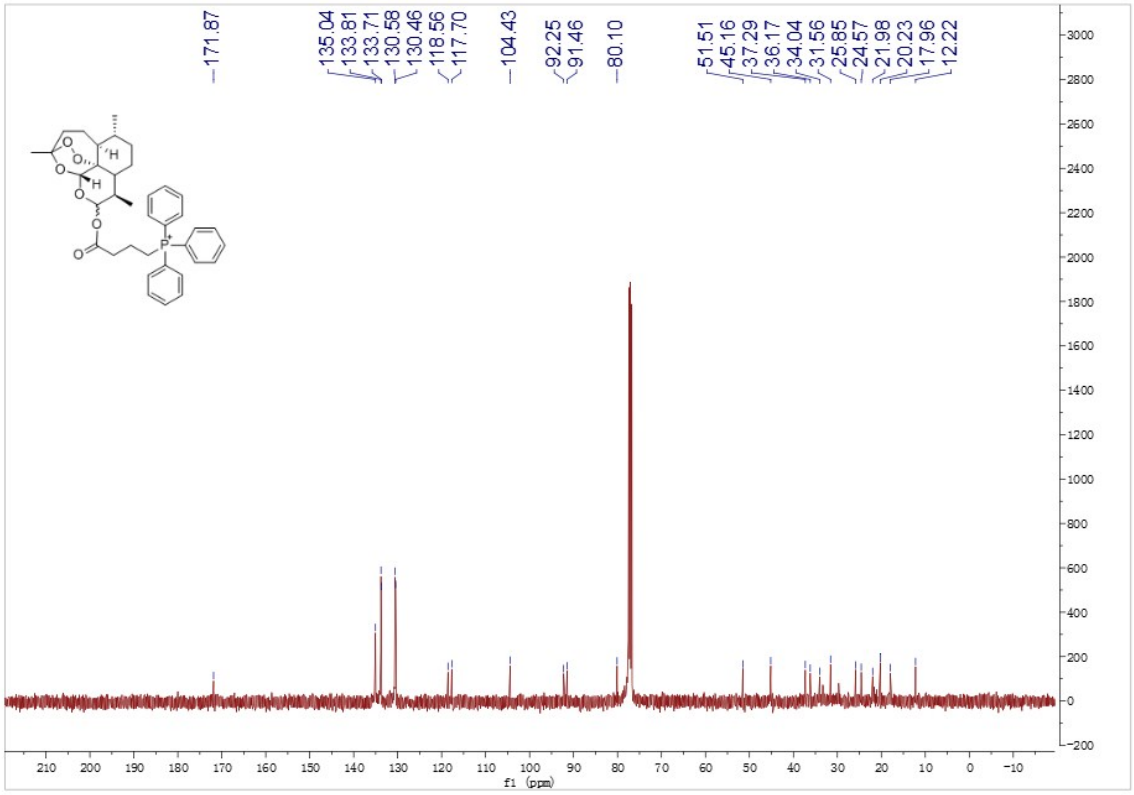

Fig. S33 ^{13}C NMR spectrum of compound **8**